NUCLEAR SCIENCE AND ENGINEERING: 79, 85-98 (1981)

The Variation of the Resonance Component of the Doppler Coefficient with Depletion of the Fissile Component of Reactor Fuel

A. Radkowsky

Tel-Aviv University, School of Engineering
Ramal-Aviv, Tel Aviv, Israel

and

Ben-Gurion University of the Negev, Department of Nuclear Engineering
Beer-Sheva, Israel

and

A. Galperin and T. Elperin

Ben-Gurion University of the Negev, Department of Nuclear Engineering
Beer-Sheva, Israel

Received November 27, 1978
Accepted March 9, 1981

A careful study has been made of the effect of depletion of the fissile component of reactor fuel on the resonance component of the Doppler reactivity coefficient (DRC) for a lattice typical of a boiling water reactor (BWR). A parallel investigation has been carried out for both uranium- and thorium-based fuels.

It is found that there are three principal effects, as follows, the first two of which tend to decrease the magnitude of the resonance component of the DRC and the third to increase it:

1. direct competition of fission product absorption with that of the fertile isotopes

2. overlapping of the fission product resonances with those of the fertile isotopes

3. in uranium only, the formation of a large saturating resonance in ^{240}Pu.

As a result, in uranium-based fuels the resonance component of the DRC changes very little with depletion of the fissile isotope, while in thorium-based fuels there is a significant decrease in magnitude. Our results cannot be applied directly to a BWR since this would require consideration of the depletion history and void distribution over the entire core.

The burnup selected for the uranium fuel was 35 000 MWd/ton, in line with current practice. In this material, effect 3 above is close to its maximum value while effects 1 and 2 increase with further burnup. Thus, it is also true that for extended burnup of uranium fuels, as are now being considered by the U.S. Department of Energy, the resonance component of the DRC is expected to decrease in magnitude.

INTRODUCTION

The variation of the Doppler reactivity coefficient (DRC) with depletion of the fissile constituent of reactor fuel is important because such variations can significantly affect reactor safety and control. In this paper, a careful study was made of the effect of such depletion on the temperature variation of the resonance absorption, the most important component of the DRC, taking into account some processes

0029-5639/81/0009-0085$02.00/0

apparently not previously considered in the literature. For the present we confine our attention to light water boiling water reactors (BWRs) in which the operation of the Doppler coefficient is particularly important. A parallel investigation was carried out for both uranium- and thorium-based fuels.

Conventionally, the DRC results mainly from the effects of temperature change on the saturated isolated resonances that occur in the lower epithermal energy region, customarily designated as energy group 3 in a four-group model, in the range from just above thermal to ~5000 eV. A saturated resonance for a heterogeneous absorber is defined as one having sufficient atom density and microscopic cross section to absorb essentially all neutrons incident at the energies in the neighborhood of the resonance peak. In general, as the temperature rises the resonance broadens so that there is less absorption at the peak and more in the wings of the resonance.

The peak is still high enough to absorb essentially all incident neutrons of that energy, while the absorption at the resonance wings has increased sufficiently to absorb many neutrons that formerly would have escaped capture. Thus, there is a net increase in effective absorption. In reactor fuels of low fissile-element content, most of the DRC at the beginning-of-life (BOL) results from broadening of the resonances in the fertile materials, ^{238}U and thorium.

During reactor operation, a large number of new isotopes are produced in the core together with a reduction in the density of some, principally the fissile fuel and burnable poisons. As a result, a large number of new resonances appear in group 3. The DRC is affected in several ways. First of all, the neutron flux distribution within group 3 is modified, so that the relative importance as well as the overall magnitude of the contributions of the original resonances to the DRC is changed and mostly reduced. Second, a number of the new resonances rapidly approach saturation, particularly ^{240}Pu, thus producing additional contributions to the DRC. Third, some of the new resonances are located within the wings of the original resonances, so as to overlap with the temperature-increased absorption cross section in the wing regions. This tends to result in a decrease in the DRC. To our knowledge, this paper contains the first treatment of the overlap effect.

In this investigation, the RABBLE code[1] was found to be an indispensable tool, since by its extremely narrow group structure, it permits interferences and overlapping effects between resonances to be taken into account. A more recent version of this code,[2] RABBLE-2, uses an exact treatment for slowing down, thus eliminating a source of error in the original RABBLE code in the treatment of extremely large absorption.

ILLUSTRATION OF DEPLETION-PRODUCED INTERFERENCES WITH TEMPERATURE BROADENING OF FERTILE MATERIAL RESONANCES

To illustrate the point, we have chosen the 20.9-eV resonance of ^{238}U and the 21-, 22-, and 23-eV doublet of ^{232}Th. Figures 1 and 2 show the RABBLE-computed flux distributions, at the BOL and at the end-of-life (EOL) in a typical BWR cell, for these two resonances, respectively. For uranium, the isotopes ^{235}U, $^{239,240,241,242}Pu$, ^{244}Cm, ^{99}Tc, ^{147}Pm, and ^{133}Cs are taken into account and ^{235}U, ^{233}U, ^{233}Pa, ^{147}Pm, ^{99}Tc, and ^{133}Cs are accounted for in the thorium case. Figure 3 shows the flux distributions at BOL for the 20.9-eV resonance of ^{238}U both at 300 and at 1200 K fuel temperatures. Figure 4 shows the flux distributions at these two temperatures at EOL. Note that in Fig. 4 the change of the flux with temperature in the wings of the resonances is much reduced as compared with the BOL case, shown in Fig. 3. This is a reflection of the fact that the effective absorption in the wings of the resonance changes much less with temperature, thus reducing the contribution of the resonance to the DRC. Figures 5 and 6 give a corresponding illustration for the 21- and 23-eV doublet of ^{232}Th.

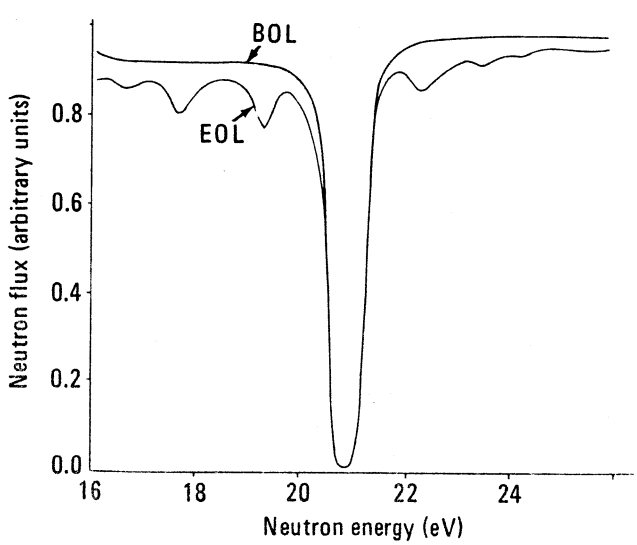

Fig. 1. Neutron flux in the vicinity of 20.9-eV resonance ^{238}U. Values at the beginning of the core life (BOL) and at the end (EOL) are shown.

[1]P. H. KIER and A. A. ROBBS, "RABBLE, A Program for Computation of Resonance Absorption in Multiregion Reactor Cells," ANL-7326, Argonne National Laboratory (1967).

[2]R. GOLDSTEIN, Combustion Engineering, Private Communication (1977).

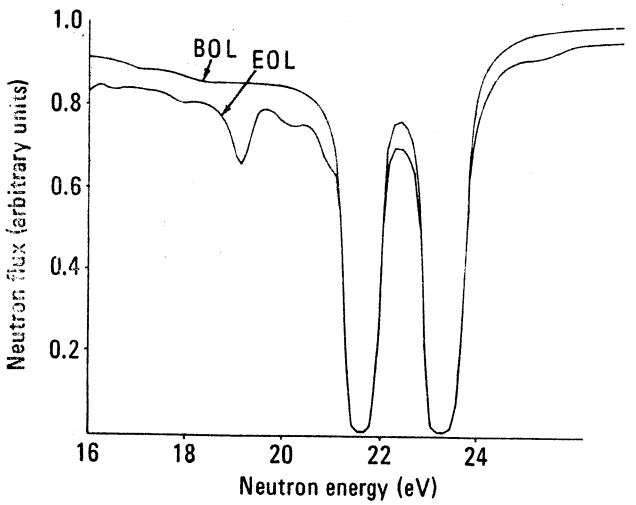

Fig. 2. Neutron flux in the vicinity of the resonance doublet of ^{232}Th.

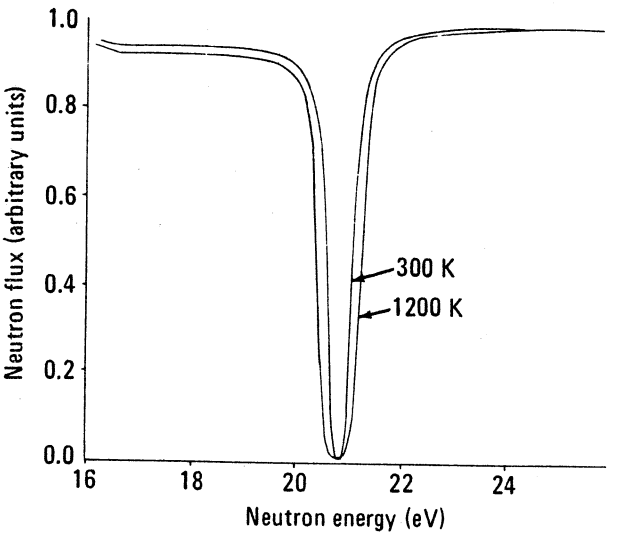

Fig. 3. Neutron flux at the isolated 20.9-eV resonance of ^{238}U at the BOL at two temperatures.

To evaluate the effects described above, detailed calculations of a resonance absorption were performed by the RABBLE-2 code for uncontaminated ^{238}U and for uranium fuel having the composition expected at the EOL. Similar calculations were done for thorium fuel.

Calculations were performed for two temperatures (1200 and 1800 K) in the 16- to 28-eV energy region. Accumulated absorption probabilities P_a for those cases are presented in Table I, where

$$P_a = \frac{\sum_m \sum_i \sum_j R_{ij}^m \Delta U_f}{\sum_m \sum_j \xi_m N_{mk} \sigma_{p,m} \Delta \Delta_j}, \qquad (1)$$

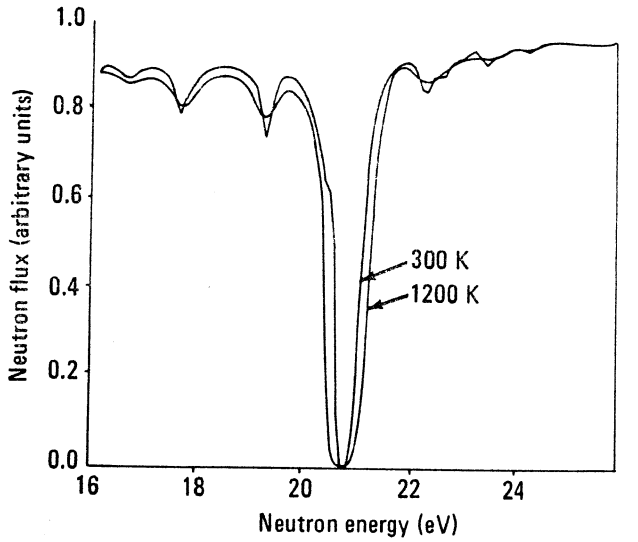

Fig. 4. Neutron flux at the 20.9-eV resonance of ^{238}U at the EOL at two temperatures.

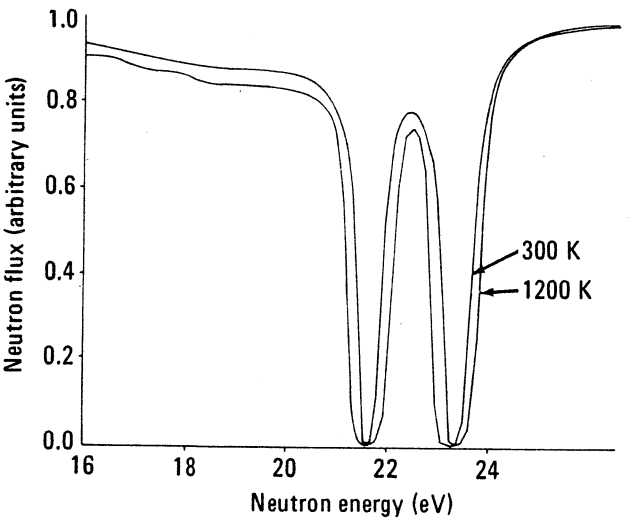

Fig. 5. Neutron flux at the isolated resonance doublet of ^{232}Th at the BOL at two temperatures.

where

ξ_m = average lethargy increment per collision for material m

$\sigma_{p,m}$ = potential scattering cross section for material m

R_{ij}^m = reaction rate for process Z in material m for fine group i and region j (i.e., the number of neutron absorptions per unit volume per unit time)

ΔU_f = lethargy width of group i

TABLE I

Absorption Probabilities for 16- to 28-eV Energy Region

Composition	P_a at T = 1200 K	P_a at T = 1800 K	$\Delta P_a = P_a(1800\ \text{K}) - P_a(1200\ \text{K})$
Clean uranium	0.03145	0.03458	0.00313
Uranium EOL	0.04765	0.05042	0.00277
Clean thorium	0.06429	0.06978	0.00549
Thorium EOL	0.08286	0.08774	0.00488

$\Delta\Delta_j$ = area of region j

N_{mk} = atom density of material m in composition k.

Table I shows the decrease of the change of absorption probabilities, which are proportional to the resonance integrals, with increasing temperature as a result of fission products and actinide resonances interfering with the resonances of fertile materials.

For the calculation of the time-dependent number densities of the nuclides created by the fission process, the CINDER code[3] was used. The CINDER code is a general one-point program that calculates the time-dependent concentrations of nuclides following irradiation in a specified time-dependent flux. The cell characteristics, calculated by the WIMS code,[4] were used as input data for the CINDER calculations. The cell-averaged cross sections in the resonance region (5.5 keV to 0.625 eV) were calculated for the compositions at BOL and at EOL and at two different fuel temperatures. For these calculations, the RABBLE-2 code[2] was used. The RABBLE-2 code allows the explicit representation of up to 16 resonant absorbers, which must be chosen from the results of the depletion calculations.

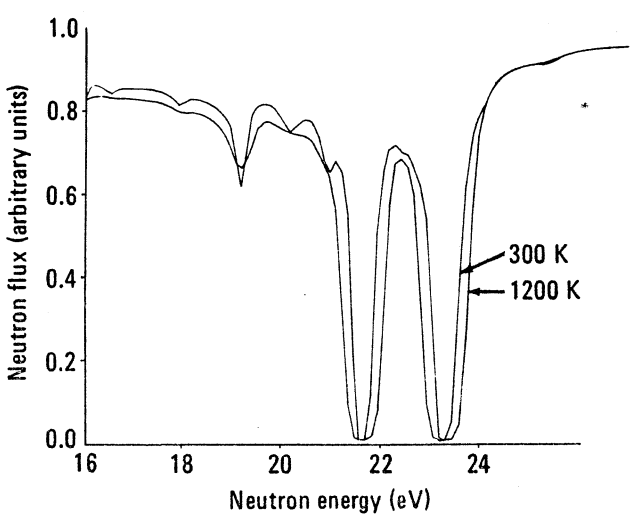

Fig. 6. Neutron flux at the resonance doublet of ^{232}Th at the EOL at two temperatures.

ISOTOPIC COMPOSITION OF THE DEPLETED FUEL

As a reference case in this work, two unit cells were chosen appropriate to a BWR: one for a 2.8 wt% ^{235}U–97.2 wt% ^{238}U mixture and the other for 2.8 wt% ^{235}U with ^{232}Th. Some basic data for the unit cells chosen are

Fuel material	UO_2 or ThO_2
Pellet diameter, cm	1.041
^{235}U content, wt%	2.8
Rod-to-rod pitch, cm	1.615
Average void content, %	40.

Depletion calculations were performed by CINDER in four energy groups:

Group	Upper Energy Limit
1	10 MeV
2	0.821 MeV
3	5.53 keV
4	0.625 eV

For both the uranium and thorium cells, the calculations accounted for the spectrum changes during lifetime. The depletion was carried out in

[3]T. R. ENGLAND, "CINDER–A One-Point Depletion and Fission Product Program," WAPD-TM-334, Bettis Atomic Power Division (Jan. 1965).

[4]J. R. ASKEW, F. I. FAYERS, and P. B. KEMSHELL, *J. Br. Nucl. Eng. Soc.*, **5**, 564 (1968).

100-h time steps with readjustment of group ratios every 7000 h. The results of these calculations were compared with the results of similar calculations performed in a constant spectrum. In the uranium case, the difference in the results for the individual isotope number densities does not exceed 5% and for the thorium case they do not exceed 1%. These differences give an indication of the appropriate choice of the number of time steps in depletion calculations. The effects of radial variation of the ^{240}Pu concentration and of the temperature rise within a fuel rod were computed to be quite small.

Fuel burnup in these calculations was taken to be ~35 000 MWd/tonne for uranium and 40 000 MWd/tonne for thorium. A comparison of the thorium and uranium fuels shows that the reactivity rundown during depletion is flatter in thorium. The parasitic capture of the slowly saturating fission products is calculated to be 20 to 30% less for ^{233}U than for ^{239}Pu and ^{241}Pu (see Tables II and III). In addition, the larger value of the number of neutrons created per fission absorbed, η, of ^{233}U compared with other fissile isotopes in the thermal and eipthermal group causes the conversion ratio for thorium fuel to be higher than for comparable uranium. To obtain a comparable loss of reactivity with depletion, a somewhat higher burnup of 40 000 MWd/tonne was utilized for the thorium fuel. The formulation of depletion and fission product chains and the basic fission product nuclide data for sets of 12 fission product chains were based on the Electric Power Research Institute EPRI-CINDER code.[5] A 12-chain set used in this work contains 38 fission products, with one pseudo-chain accurately reproducing the absorption buildup of the basic 84 chains. Results of the depletion calculations are presented in Table II for the uranium cell and in Table III for the thorium cell and include the list of the 13 elements with the largest absorption in the resonance region. The burnup values are close to the maximum to be found in the core. However, the U.S. Department of Energy is proposing much higher burnup to improve uranium utilization.

TABLE II

EOL Composition of the Uranium Fuel

Subgroup	Element	Density (10^{24} atom/cm^3)
1	^{235}U	0.1970×10^{-3}
2	^{236}U	0.7610×10^{-4}
3	^{238}U	0.2108×10^{-1}
4	^{239}Pu	0.765×10^{-4}
5	^{240}Pu	0.470×10^{-4}
6	^{241}Pu	0.340×10^{-4}
7	^{242}Pu	0.1720×10^{-4}
8	^{244}Cm	0.2010×10^{-5}
9	^{99}Tc	0.4490×10^{-4}
10	^{145}Nd	0.2460×10^{-4}
11	^{147}Pm	0.4890×10^{-5}
12	^{103}Rh	0.1950×10^{-4}
13	^{131}Xe	0.1490×10^{-4}

TABLE III

EOL Composition of the Thorium Fuel

Subgroup	Element	Density (10^{24} atom/cm^3)
1	^{232}Th	0.1929×10^{-1}
2	^{233}Pa	0.213×10^{-4}
3	^{233}U	0.320×10^{-3}
4	^{234}U	0.777×10^{-4}
5	^{235}U	0.667×10^{-4}
6	^{236}U	0.794×10^{-4}
7	^{237}Np	0.137×10^{-6}
8	^{103}Rh	0.942×10^{-5}
9	^{131}Xe	0.1680×10^{-4}
10	^{133}Cs	0.491×10^{-4}
11	^{147}Pm	0.388×10^{-5}
12	^{145}Nd	0.306×10^{-5}
13	^{154}Eu	0.840×10^{-5}

Initial fuel compositions in the CINDER calculation of the uranium cell were ^{235}U density = 0.6203×10^{21} atom/cm^3 and ^{238}U density = 0.2167×10^{23} atom/cm^3, and for the thorium cell they were ^{235}U density = 0.5900×10^{21} atom/cm^3, ^{232}Th density = 0.2038×10^{23} atom/cm^3.

The elements listed in Tables II and III are the important absorbers. They were chosen to be treated explicitly in resonance absorption calculations. First, the elements with the highest number densities and resonance absorption cross sections were selected using the GRAF code[6] in the following way: Various resonance shapes were generated from Evaluated Nuclear Data File (ENDF)/B-IV tapes (file 2 only) of Breit-Wigner parameters, and the generated microscopic cross sections were multiplied by appropriate number densities and and plotted.

Those elements whose resonances are large enough and/or are situated on the wings of the fertile material resonances so as to have an appreciable overlapping effect were marked as "important" and are included in Tables II and III. An example of such a graphical analysis for the uranium cell is shown in Fig. 7.

[5]T. R. ENGLAND, W. B. WILSON, and M. G. STAMATELATOS, "Fission Product Data for Thermal Reactors," LA-6745-MS and LA-6746-MS, Los Alamos National Laboratory (Dec. 1976).

[6]J. J. WAGSCHAL, Hebrew University, Private Communication (1977).

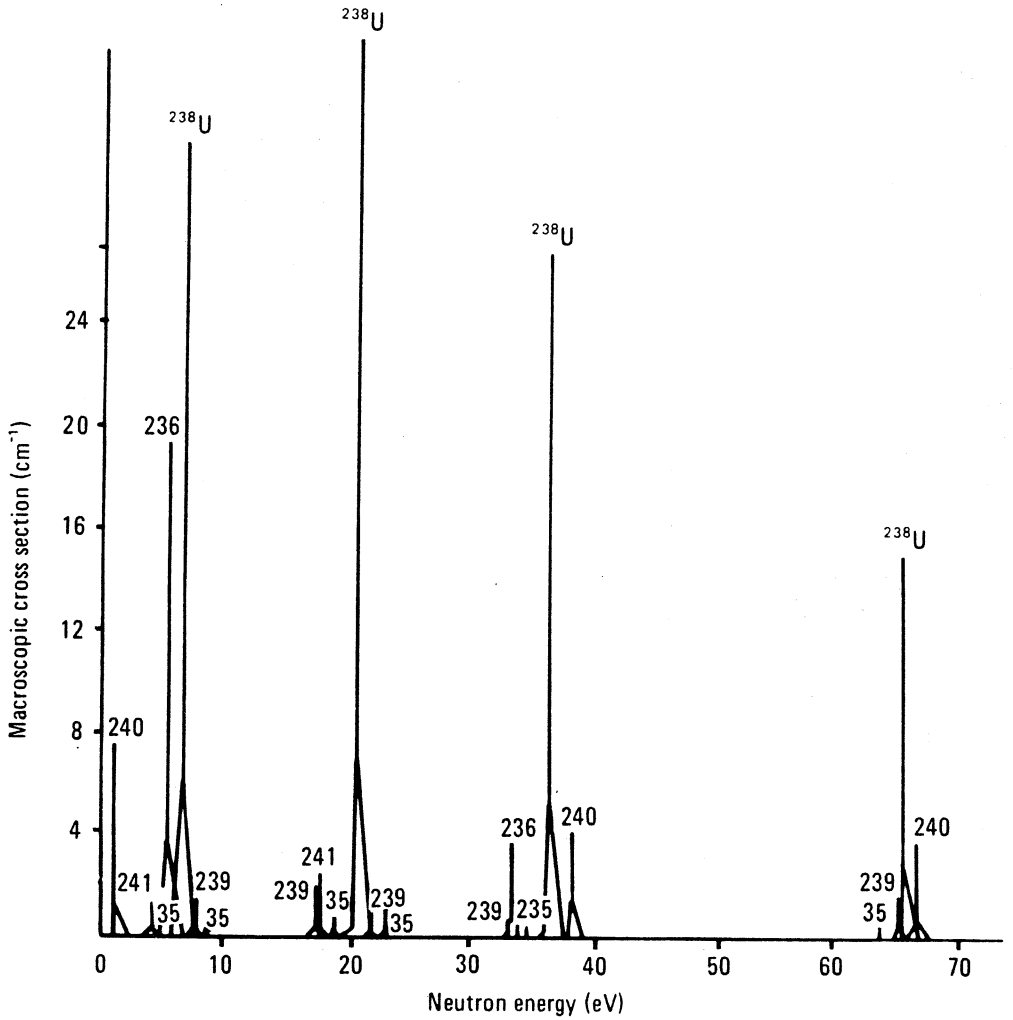

Fig. 7. Resonance structure at the end of core life. For all resonances except those of ^{238}U and the 1.06-eV resonance of ^{240}Pu, multiply cross-section scale by 10^{-1}.

The total macroscopic neutron absorption cross sections of all the fission products of the uranium fuel (including those of Table III), found by summing the individual values, are

1. Epithermal absorption = 0.185×10^{-1} (cm^{-1})
2. Thermal absorption = 0.692×10^{-1} (cm^{-1}).

The total macroscopic neutron absorption cross section of the fission products in the thorium cell are

1. Epithermal = 0.125×10^{-1} cm^{-1}
2. Thermal = 0.560×10^{-1} cm^{-1}.

In the case of a $1/v$ behavior of the absorption cross section of the fission products, the epithermal cross section can be calculated by the formula[3]

$$\Sigma_{epi} = \Sigma_{th} \frac{(0.0253)^{1/2} \int_{0.625}^{5530} \frac{dE}{E^{3/2}}}{\int_{0.625}^{5530} \frac{dE}{E}} = 0.04\Sigma_{th} \quad . \quad (2)$$

The $1/v$ value of the epithermal cross section is ~4% of the thermal cross section. Comparing this with the values calculated by CINDER for the uranium and thorium cells (where epithermal absorption is more than 20% of the thermal absorption), it is clear that the non-$1/v$ behavior of the fission product cross section must be taken into account, otherwise the absorption of the fission product in the resonance region will be substantially underestimated.

RESONANCE ABSORPTION CALCULATIONS

The calculations of the resonance absorption in the fuel for both cells and the generation of the resonance cross sections for BOL- and the EOL-fuel compositions for the two temperatures (800 and 1200 K) were performed by the RABBLE-2 code. The basic quantities computed are the cell-averaged neutron flux for the broad group I:

$$\Phi_I = \frac{\sum_i \sum_j \Phi_{ij} \Delta U_f}{\sum_i \sum_j \Delta U_f \Delta \Delta_j} , \quad (3)$$

and the cell-averaged macroscopic cross section for process Z and group I:

$$z\bar{\Sigma}_I = \frac{\sum_m \sum_i \sum_j R_{ij}^m \Delta U_f}{\sum_i \sum_j \Phi_{ij} \Delta U_f} , \quad (4)$$

where, in addition to the definitions given above, Φ_{ij} is the neutron flux in group i and region j.

The RABBLE-2 code calculations were performed in 17 broad energy subgroups (with the structure given in Table IV), which were divided into ~17 000 fine-structure groups.

The elements listed in Tables II and III for the uranium and thorium cells were taken into account explicitly, i.e., as resonant absorbers. A set of resonance parameters for each element was prepared from file 2 of the ENDF/B-IV library, neglecting smooth cross-section data from file 3. The thermal neutron absorption of all other elements produced during the fuel burnup was taken into account by introducing a fictitious element into the EOL composition as a nonresonance material. The number density of this element was chosen according to the accumulated fission density, and the microscopic cross section was fitted so as to keep the total macroscopic absorption cross section equal to that calculated by CINDER. For the (epithermal) resonance energy region, an additional constant background absorption was prescribed for ^{235}U (or for ^{233}U in the case of thorium), following the same criteria as for the thermal region. Four RABBLE-2 calculations were carried out to generate resonance cross sections for BOL and EOL compositions at two temperatures, 800 and 1200 K. The results of these calculations are presented in Tables V and VI for uranium fuel and in Tables VII and VIII for thorium fuel.

TABLE IV

The RABBLE Energy Subgroups

Broad Subgroup	Upper Energy Limit (eV)	Lethargy Width	Number of Fine-Structure Groups
1	5.5250+03[a]	0.45200	904
2	3.5159+03	0.45200	904
3	2.2373+03	0.45200	904
4	1.4237+03	0.45200	904
5	9.0600+02	0.00400	1808
6	3.6688+02	0.90400	1808
7	1.4857+02	0.67800	1356
8	7.5417+01	0.45200	904
9	4.7992+01	0.55100	1102
10	2.7661+01	0.55100	1102
11	1.5943+01	0.48000	960
12	9.8654+00	0.90400	1808
13	3.9950+00	0.19200	384
14	3.2971+00	0.23800	476
15	2.5988+00	0.21400	428
16	2.0981+00	0.60200	1204
17	1.1492+00[b]	0.61000	1220

[a]Read as 5.5250×10^3.
[b]The lower limit of group 17 is 6.2440×10^{-1} eV.

The results shown in Tables V and VI for the uranium cell reveal that the main temperature broadening of the resonance cross sections at BOL occurs in subgroups 5 through 12, i.e., from 5 to 900 eV; there is no broadening effect in subgroups 13 through 17 for BOL composition because the lowest ^{238}U resonance is at 6.67 eV. For the EOL composition, the situation is changed substantially in the lower subgroups where the main resonance of ^{240}Pu, at 1.06 eV, is situated. The last column in these tables is defined as

$$\Delta\Sigma_a = \Sigma_a(T = 1200 \text{ K}) - \Sigma_a(T = 800 \text{ K}) . \quad (5)$$

The values of $\Delta\Sigma_a$ in various subgroups and compositions (see Tables V and VI and Fig. 8) indicate the changes of cross section as a function of energy.

Generally, the temperature changes for EOL, as compared with BOL, are decreased in higher subgroups 1 through 11 and increased in lower subgroups 12, 15, 16, 17, primarily the ^{240}Pu effect.

The corresponding results for thorium are shown in Tables VII and VIII and Fig. 9. The values of $\Delta\Sigma_a$ generally decrease with burnup. The largest change occurs in subgroup 10, where the resonance

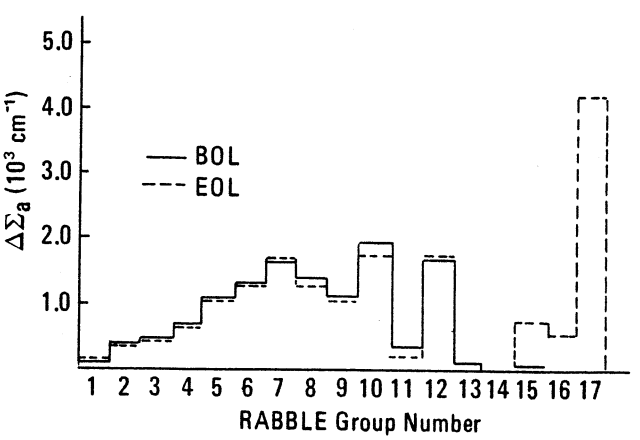

Fig. 8. Change in macroscopic absorption cross sections, for a uranium cell, due to temperature change from 800 to 1200 K.

TABLE V

Broad Subgroup Fluxes and Cross Sections for Uranium Having BOL Composition

Subgroup	T = 800 K		T = 1200 K		$\Delta\Sigma_a$ (10^{-3} cm^{-1})
	Flux (arbitrary units)	Σ_a (cm^{-1})	Flux (arbitrary units)	Σ_a (cm^{-1})	
1	0.9698	0.01066	0.9695	0.01073	0.07
2	0.9504	0.00950	0.9567	0.00986	0.36
3	0.9468	0.01068	0.9451	0.01114	0.46
4	0.9272	0.01410	0.9243	0.01481	0.71
5	0.8963	0.017621	0.8914	0.01873	1.11
6	0.8528	0.02158	0.8454	0.02292	1.34
7	0.7969	0.03198	0.7876	0.03371	1.73
8	0.7575	0.03366	0.7473	0.03505	1.39
9	0.6890	0.05518	0.6799	0.05627	1.09
10	0.6259	0.06825	0.6156	0.07018	1.93
11	0.6617	0.02313	0.6528	0.02348	0.35
12	0.5278	0.08020	0.5181	0.08189	1.69
13	0.5784	0.01636	0.5696	0.01642	0.06
14	0.5813	0.01113	0.5725	0.01111	−0.02
15	0.5870	0.00618	0.5780	0.006272	0.09
16	0.5778	0.01042	0.5690	0.01039	−0.03
17	0.5641	0.01172	0.5556	0.01171	−0.01

TABLE VI

Broad Subgroup Fluxes and Cross Sections for Uranium Having EOL Composition

Subgroup	T = 800 K		T = 1200 K		$\Delta\Sigma_a$ (10^{-3} cm^{-1})
	Flux (arbitrary units)	Σ_a (cm^{-1})	Flux (arbitrary units)	Σ_a (cm^{-1})	
1	0.9723	0.00977	0.9720	0.00985	0.08
2	0.9615	0.00859	0.9604	0.00894	0.35
3	0.9522	0.00941	0.9505	0.00985	0.44
4	0.9349	0.01239	0.9319	0.01309	0.7
5	0.9067	0.01573	0.9018	0.01682	1.09
6	0.8679	0.01905	0.8604	0.02036	1.31
7	0.8142	0.02928	0.8047	0.03102	1.74
8	0.7796	0.02913	0.7694	0.03039	1.26
9	0.7147	0.04935	0.7054	0.05039	1.04
10	0.6548	0.06170	0.6445	0.06341	1.71
11	0.6695	0.02970	0.6608	0.02992	0.22
12	0.5323	0.08916	0.5228	0.09088	1.72
13	0.5868	0.01362	0.5781	0.01364	0.02
14	0.5611	0.03439	0.5528	0.03438	−0.01
15	0.5739	0.01206	0.5643	0.01282	0.76
16	0.5498	0.029390	0.5409	0.02996	0.57
17	0.4019	0.11001	0.3909	0.11422	4.21

TABLE VII

Broad Subgroup Fluxes and Cross Sections at 800 and 1200 K for Thorium Having BOL Composition

Subgroup	T = 800 K		T = 1200 K		
	Flux (arbitrary units)	Σ_a (cm^{-1})	Flux (arbitrary units)	Σ_a (cm^{-1})	$\Delta\Sigma_a$ (10^{-3} cm^{-1})
1	0.9962	1.579–03	0.9960	1.624–03	0.045
2	0.9771	7.207–03	0.9762	7.535–03	0.328
3	0.9593	9.589–03	0.9571	1.019–02	0.601
4	0.9513	1.077–02	0.9485	1.148–02	0.710
5	0.9266	1.236–02	0.9210	1.355–02	1.19
6	0.8773	2.064–02	0.8655	2.325–02	2.61
7	0.8545	1.657–02	0.8412	1.838–02	1.81
8	0.7677	4.819–02	0.7524	5.099–02	2.80
9	0.8025	1.671–02	0.7911	1.679–02	0.080
10	0.6596	7.487–02	0.6409	8.003–02	5.130
11	0.7216	1.902–02	0.7076	1.934–02	0.320
12	0.7052	1.623–02	0.6915	1.640–02	0.170
13	0.7090	1.018–02	0.6955	1.023–02	0.050
14	0.7104	6.436–03	0.6969	6.416–03	−0.02
15	0.7173	2.248–03	0.7035	2.339–03	0.091
16	0.7082	6.518–03	0.6948	6.500–03	−0.018
17	0.6961	7.408–03	0.6829	7.404–03	−0.004

TABLE VIII

Broad Subgroup Fluxes and Cross Sections for Thorium Having EOL Composition

Subgroup	T = 800 K		T = 1200 K		
	Flux (arbitrary units)	Σ_a (cm^{-1})	Flux (arbitrary units)	Σ_a (cm^{-1})	$\Delta\Sigma_a$ (10^{-3} cm^{-1})
1	0.9962	1.558–03	0.9961	1.599–03	0.041
2	0.9778	6.999–03	0.9769	7.303–03	0.304
3	0.9604	9.344–03	0.9584	0.902–03	0.558
4	0.9522	1.059–02	0.9496	1.126–02	0.670
5	0.9272	1.239–02	0.9219	1.352–02	1.130
6	0.8757	2.139–02	0.8643	2.395–02	2.560
7	0.8497	1.792–02	0.8369	1.969–02	1.770
8	0.7807	4.068–02	0.7655	4.347–02	2.790
9	0.8124	1.429–02	0.8012	1.433–02	0.040
10	0.6690	7.208–02	0.6509	7.682–02	4.74
11	0.6993	3.271–02	0.6865	3.292–02	0.210
12	0.6459	4.505–02	0.6329	4.585–02	0.800
13	0.6415	2.381–02	0.6291	2.374–02	−0.070
14	0.6516	1.362–02	0.6390	1.371–02	0.090
15	0.5955	5.176–02	0.5837	5.202–02	0.260
16	0.5299	7.1218–02	0.5197	7.122–02	0.002
17	0.5643	2.009–02	0.5533	2.016–02	0.070

doublet (11.23 eV) is situated, and other large changes occur in subgroups 5 through 8.

Absorption cross sections from Tables V through VIII were averaged over the entire resonance region[1] by the formula

$$\Sigma_{a3} = \frac{\sum_{i=1}^{17} \Sigma_{ai} \Phi_i \Delta U_i}{\sum_{i=1}^{17} \Phi_i \Delta U_i} . \quad (6)$$

The values Σ_{ai} and Φ_i are cell-averaged subgroup cross sections and fluxes, calculated by RABBLE-2. The results of this averaging are presented in Table IX.

The last column in Table IX shows the fractional change in the macroscopic resonance absorption cross section (group 3) from 800 to 1200 K, $\Delta\Sigma_a/\Sigma_a$ averaged over the flux distribution in group 3 as calculated by RABBLE, and averaged spacewise over the cell. Note that there is a decrease in the fractional change of group 3 absorption cross section due to fuel temperature from BOL to EOL, and that the decrease is much greater in the thorium case.

TABLE IX

Resonance Absorption Cross Sections of Uranium and Thorium Cells Averaged over a Unit Cell and over Energy Group 3

Composition	Average Resonance Absorption, Σ_a Cross Section (cm^{-1})		Fractional Change with Temperature, $\Delta\Sigma_a/\Sigma_a$
	T = 800 K	T = 1200 K	
Uranium			
BOL	0.02672	0.02753	0.0300
EOL	0.03117	0.03209	0.0296
Thorium			
BOL	0.01700	0.01799	0.0584
EOL	0.02471	0.02570	0.0402

CALCULATION OF REACTION RATES

The effects on cell multiplication factors and Doppler coefficients can be derived from a comparison of the values of the absorption reaction rates for BOL and EOL compositions.

The changes of the reaction rates caused by the temperature changes for both compositions for the uranium cell are presented in Table X and Fig. 10, where

$$\Delta R_i = R_i(1200\ \text{K}) - R_i(800\ \text{K}) , \quad (7)$$

and where $R_i = \Phi_i \Sigma_i \Delta U$. Similar data for the thorium cell are presented in Table XI and Fig. 11. For each element the changes in reaction rates are quite similar to those for the corresponding macroscopic absorption cross sections.

COMPARISON WITH THE TECHNION HAMMER CODE SYSTEM (OZMA)

The results obtained by the procedure described above were compared with the results obtained by

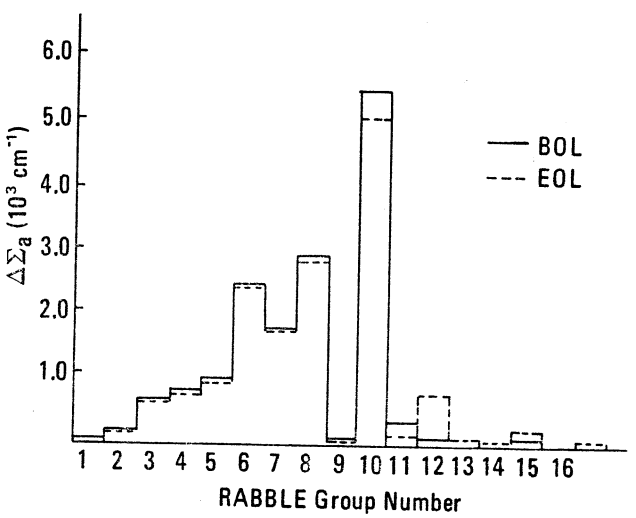

Fig. 9. Change in macroscopic absorption cross sections, for a thorium cell, due to temperature change from 800 to 1200 K.

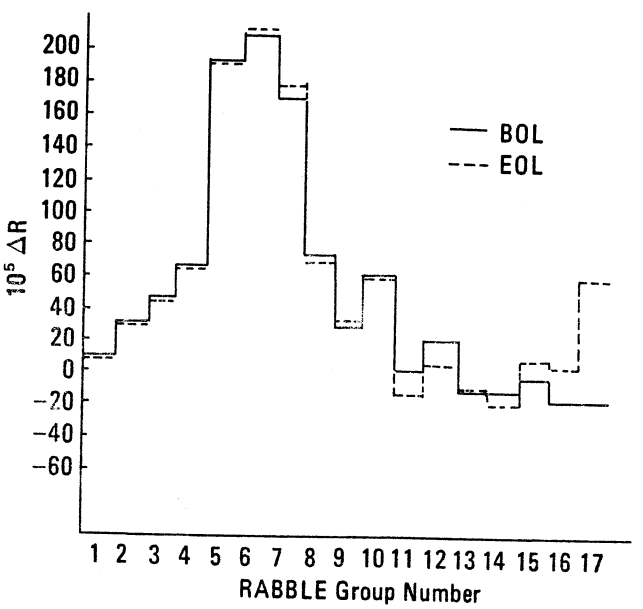

Fig. 10. Change in reaction rate, for a uranium cell, due to temperature change from 800 to 1200 K.

TABLE X

Changes in Reaction Rates with Temperature Change (800 to 1200 K) for Uranium Cells of Two Compositions

Subgroup	BOL $\Delta R_i \times 10^5$ $(cm^3 \cdot s)^{-1}$	EOL $\Delta R_i \times 10^5$ $(cm^3 \cdot s)^{-1}$
1	7.9	7.7
2	35.6	34.6
3	44.5	43.9
4	65.7	65.2
5	193.4	193.0
6	207.9	211.6
7	170.0	180.0
8	75.0	71.0
9	30.0	35.0
10	63.0	61.0
11	3.0	−13.0
12	22.0	12.0
13	−6.0	−5.0
14	−6.0	−16.0
15	1.0	16.0
16	−15.0	6
17	−15.0	64.0
Total	877	967

TABLE XI

Changes in Reaction Rates with Temperature Change for Thorium Cells of Two Compositions (ΔT = 800 to 1200 K)

Subgroup	BOL $\Delta R_i \times 10^5$ $(cm^3 \cdot s)^{-1}$	EOL $\Delta R_i \times 10^5$ $(cm^3 \cdot s)^{-1}$
1	4.80	4.40
2	33.5	31.5
3	58.9	55.1
4	69.6	65.2
5	218.9	208.9
6	432.3	420.4
7	209.0	200.9
8	147.0	163.0
9	−17.0	−16.0
10	248.0	231.0
11	−4.0	−32.0
12	−22.0	−16.0
13	−4.0	−15.0
14	−6.0	−6.0
15	2.0	−24.0
16	−14.0	−104.0
17	−15.0	−27.0
Total	1340	1140

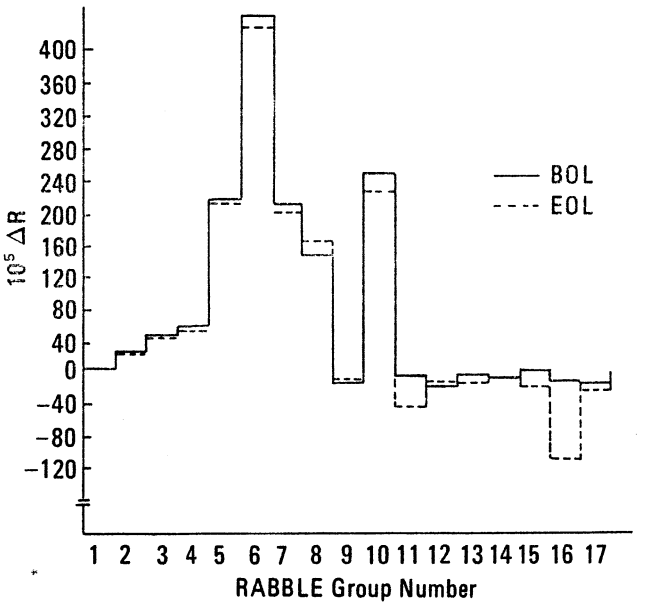

Fig. 11. Change in reaction rate, for a thorium cell, due to temperature change from 800 to 1200 K.

the Technion Hammer code[7] for the BOL and EOL compositions of uranium fuel. At present the Technion code is limited in the number of resonant isotopes that can be handled explicitly with resonance profiles. Therefore, in the comparison only the isotopes ^{235}U, ^{238}U, ^{239}Pu, ^{240}Pu, ^{241}Pu, ^{148}Nd, and ^{147}Pm from Table II were treated explicitly. The results of the comparison are presented in Tables XII and XIII.

The results are in reasonable agreement, especially if one takes into account the completely different cross-section representation in the Ben-Gurion and the Technion calculations. In the Ben-Gurion calculations, resonance cross sections were calculated by the one-level Breit-Wigner formalism with the full set of ENDF/B-IV resonance parameters. In the Technion calculations, tabulated resonance profiles were utilized. It should be noted in Table XII that the fractional change in the resonance absorption cross section with temperature, in the 800 to 1200 K range, is smaller for the BOL composition than for the EOL composition. This is true for both sets of calculations. On the other hand, when the calculations include the more complete set of resonant isotopes (those listed in Table II), which can be handled only by the procedures used by the Ben Gurion University group, the fractional change in the resonance absorption cross section is practically the same at EOL and BOL.

[7]J. BARHEN, W. ROTHENSTEIN, and E. TAVIV, "The Hammer Code System," NP-565, Electric Power Research Institute (1978).

TABLE XII

Comparison of the Ben-Gurion University Results with the Technion Hammer Code on Cell-Averaged Macroscopic Absorption Cross Sections (cm^{-1}) in the Resonance Energy Region

Cross Section	Ben-Gurion University	Technion
Σ_a^{BOL} (800 K)	0.02672	0.02700
Σ_a^{BOL} (1200 K)	0.02753	0.02788
Σ_a^{EOL} (800 K)	0.02900	0.02848
Σ_a^{EOL} (1200 K)	0.02994	0.02939
$\Delta\Sigma_a^{BOL} = \Sigma_a^{BOL}$ (1200 K) $- \Sigma_a^{BOL}$ (800 K)	0.000811	0.000799
$\Delta\Sigma_a^{EOL} = \Sigma_a^{EOL}$ (1200 K) $- \Sigma_a^{EOL}$ (800 K)	0.000939	0.000907
$\delta^{BOL} = \Delta\Sigma_a^{BOL}/\Sigma_a^{BOL}$ (800 K)	0.0303	0.0296
$\delta^{EOL} = \Delta\Sigma_a^{EOL}/\Sigma_a^{EOL}$ (800 K)	0.0323	0.0318

TABLE XIII

Comparison of the Relative Changes in the Absorption Reaction Rates, R, Averaged over the Uranium Cell as Calculated by the Ben-Gurion University and Technion Groups

Relative Changes in Reaction Rates	Ben-Gurion University	Technion
$(\Delta R/R)^{BOL} = [R^{BOL}(1200\text{ K}) - R^{BOL}(800\text{ K})]/R^{BOL}(800\text{ K})$	0.02050	0.01940
$(\Delta R/R)^{EOL} = [R^{EOL}(1200\text{ K}) - R^{EOL}(800\text{ K})]/R^{EOL}(800\text{ K})$	0.02209	0.02145
$\delta = (\Delta R^{EOL} - \Delta R^{BOL})/\Delta R^{BOL}$	0.184	0.190

We believe that this result is attributable to interferences between the resonances of the fission products with those of the fertile material.

It will be noted that the Ben Gurion University procedure, as described in the previous sections, does not include smoothing corrections. To find the effect of these corrections, we introduce them as a constant background cross section for each of the 17 RABBLE subgroups. The corrections were generated by the ETOG code[8] from the ENDF/B-III data for the MUFT group structure and then recalculated by hand for the RABBLE group structure. The list of the corrections to the capture and fission cross sections for ^{238}U, ^{235}U, ^{239}Pu, ^{240}Pu and ^{241}Pu is presented in Table XIV.

Table XV shows the influence of the smoothing corrections in different energy subgroups. Only small changes in ΔR occur in groups where smoothing corrections are relatively large.

Table XVI gives the overall effects of including the smoothing corrections. The effects in the temperature dependence of the absorption reaction rates and macroscopic cell-averaged absorption cross sections are negligible. Reaction rates and cross sections differ from the case without smoothing corrections by ~1% for R and 2% for Σ_a, but the temperature dependences are the same. This result was expected because smoothing corrections are temperature independent.

As a further check, using the EOL composition of the Ben-Gurion/Technion comparison, the Ben-Gurion calculation was repeated with the fission product cross sections treated as equivalent smoothed cross sections. The values in Tables XII and XIII did not change appreciably, showing that for these particular isotopes there is little interference with the resonances of the fertile isotopes.

DISCUSSION AND CONCLUSIONS

For uranium nuclear reactor fuel, in the resonance energy region, we have found little effect of the depletion of the fissile isotope on the absorption cross section and reaction rate caused by changes

[8]M. RAYMOND, "ETOG-1, A FORTRAN-IV Program to Process Data from the ENDF/B File to the MUFT, GAM and ANISN Formats," WCAP-3485-1, Westinghouse Electric Corporation, Atomic Power Department (1973).

TABLE XIV

Smoothing Corrections Generated by the ETOG-3 Code for the RABBLE Group Structure

Group	^{238}U $\sigma_c(l)$[a]	^{235}U $\sigma_c(l)$	^{235}U $\sigma_f(l)$	^{239}Pu $\sigma_c(l)$	^{239}Pu $\sigma_f(l)$	^{240}Pu $\sigma_c(l)$	^{241}Pu $\sigma_c(l)$	^{241}Pu $\sigma_f(l)$
1	0.83	1.42	4.40	2.10	2.59	1.42	1.53	5.72
2	0.46	1.82	5.25	3.04	3.04	1.07	1.96	7.19
3	0.33	2.42	6.75	3.40	3.46	0.76	2.51	8.70
4	0.25	3.72	8.25	4.37	5.76	0.83	2.54	10.68
5	0.15	4.78	12.79	7.85	8.63	0.69	4.95	16.27
6	0.097	8.77	18.97	2.83	2.40	0.32	8.14	26.44
7	0.11	11.94	20.73	20.54	0.40	0.16	11.82	36.33
8	0.02	0.01	0.39	1.70	−0.68	−0.01	10.19	37.33
9	0.14	−0.05	0.23	0.87	0.07	0.02	−0.01	−1.30
10	0.06	0.06	0.16	1.09	2.01	−0.05	−0.04	−1.97
11	0.08	0.77	1.48	1.35	3.63	−0.18	0.02	−1.59
12	0.20	0.64	0.76	0.56	4.78	−0.93	0.17	0.71
13	0.26	0.82	3.89	0.41	8.92	−2.98	0.78	8.79
14	0.23	1.35	5.87	0.94	10.93	−4.95	0.82	10.91
15	0.37	1.56	8.59	2.11	13.80	−9.21	0.96	11.39
16	0.33	2.65	10.11	6.51	21.83	52.63	1.86	15.93
17	0.85	4.13	49.41	20.76	51.85	93.16	6.83	27.68

[a]The value $\sigma_c(l)$ is the microscopic cross section in subgroup l. The subscripts c and f denote capture and fission, respectively.

TABLE XV

Comparison of the Changes in Reaction Rates due to Temperature Change from Calculations With and Without Smoothing Corrections

ΔT = 800 to 1200 K

Subgroup	With Correction $\Delta R \times 10^5$ $(cm^3 \cdot s)^{-1}$	Without Correction $\Delta R \times 10^5$ $(cm^3 \cdot s)^{-1}$
1	3	3
2	14	14
3	17	16
4	27	27
5	82	78
6	91	87
7	79	75
8	31	29
9	16	14
10	27	25
11	−6	−7
12	16	20
13	−2	−3
14	−7	−8
15	6	11
16	2	1
17	20	21

TABLE XVI

Comparison of the Total Reaction Rates, Fluxes and Macroscopic Cross Sections Calculated With and Without Smoothing Corrections

	$R = \sum_{i=1}^{17} \Sigma_{ai}\phi_i\Delta U_i$ $(cm^3 \cdot s)^{-1}$		$\phi = \sum_{i=1}^{17} \phi_i \Delta U_i$ $(n/cm^2 \cdot s)$		$\Sigma_a = \frac{R}{\phi}$ (cm^{-1})	
	T = 800 K	1200 K	800 K	1200 K	800 K	1200 K
Without smoothing corrections	0.2100	0.2141	6.7379	6.6717	0.03117	0.03209
With smoothing corrections	0.2128	0.2169	6.7206	6.6533	0.03167	0.03260

ΔR with smoothing correction = 0.0041 $(cm^3 \cdot s)^{-1}$; $\Delta\Sigma_a$ with smoothing correction = 0.00092 cm^{-1}.

ΔR without smoothing correction = 0.0041 $(cm^3 \cdot s)^{-1}$; $\Delta\Sigma_a$ without smoothing correction = 0.00093 cm^{-1}.

in temperature. Decreases in these quantities are attributed partly to the direct competition of unsaturated fission product resonances with those of ^{238}U and partly to the overlap of such fission product resonances with the wings of the ^{238}U resonances. There is a competing effect due to the buildup of ^{240}Pu, the resonances of which quickly saturate, particularly at 1.06 eV.

In thorium the situation is similar. However, since there are no new saturating resonances corresponding to those of ^{240}Pu (the ^{234}U resonances are far too weak to saturate), the predominant effects of fissile-isotope depletion act to decrease the magnitudes of the change in absorption cross section and the reaction rate with temperature. Similar decreases are expected in uranium at greater depletion.

We have not translated these results into changes in the DRC because it would be necessary to have data at more temperatures to do so accurately. Our two temperatures, 800 and 1200 K, are too widely spaced to permit obtaining an accurate derivative. Further, to be meaningful we would have to integrate over an entire core, which is outside the scope of our effort.

ACKNOWLEDGMENTS

The work for the uranium case was partly supported under contract with the U.S. Nuclear Regulatory Commission. Thanks are due to Rubin Goldstein of Combustion Engineering, Inc., for making RABBLE-2 available to us. We are greatly indebted to Wolfgang Rothenstein of Technion for invaluable assistance and consultation, and to the Electric Power Research Institute (EPRI) for permission to quote from Rothenstein's results on EPRI-sponsored research. We also appreciate consultation and assistance from Yigal Ronen of Ben Gurion University. Finally we wish to thank Yehuda Wagschal of the Hebrew University for preparing the GRAF code.